Scientific Research Publishing

Food and Nutrition Sciences, 2021, 12, 308-318
https://www.scirp.org/journal/fns
ISSN Online: 2157-9458
ISSN Print: 2157-944X

Synthesis and Characterization of Zinc Oxide and Zinc Oxide Doped with Chlorine Nanoparticles as Novel α-Amylase Inhibitors

A. Al-Arfaj Ahlam[1*], N. Abd El-Rahman Soheir[2]

[1]Department of Chemistry, College of Science, Imam Abdulrahman Bin Faisal University, Dammam, KSA
[2]Crops Technology Research Department, Food Technology Research Institute, Agricultural Research Center, Giza, Egypt
Email: *ahalarfaj@iau.edu.sa

How to cite this paper: Ahlam, A. Al-Arfaj and Soheir, N. Abd El-Rahman (2021) Synthesis and Characterization of Zinc Oxide and Zinc Oxide Doped with Chlorine Nanoparticles as Novel α-Amylase Inhibitors. *Food and Nutrition Sciences*, **12**, 308-318.
https://doi.org/10.4236/fns.2021.123024

Received: February 13, 2021
Accepted: March 26, 2021
Published: March 29, 2021

Abstract

In this study we used a chemical solution method from oxalic acid (OX. acid) and zinc acetate (ZnAc) to prepare Zinc Oxide nanoparticles (ZnONPs) and Zinc Oxide nanoparticles doped with Chlorine (Cl:ZnONPs). The characterizations (FTIR, X-ray, SEM, TEM) of ZnONPs and Cl:ZnONPs were determined. Amylase inhibitors of ZnONPs and Cl:ZnONPs also were determined. SEM indicated that the ZnONPs and Cl:ZnONPs have an average particle size of 46.65 - 74.64 nm. TEM images of the ZnONPs and Cl:ZnONPs showed the round shaped. Compounds b, d and e exhibited significant inhibitory activity against amylase enzyme (from 69.21 ± 1.44 to 76.32 ± 0.78), respectively, and were comparable with that of acarbose (86.32 ± 0.63) at 1000 µg, thereby, projecting ZnONPs and Cl:ZnONPs as α-amylase inhibitors.

Keywords

Zinc Oxide Nanoparticles, Zinc Oxide Nanoparticles Doped with Chlorine, Crystallinity, Anti-Diabetic Activity, α-Amylase Inhibitors

1. Introduction

Zinc oxide nanoparticles (ZnONPs) was an important functional oxide because it is a cheap non-toxic semiconductor and has a wide (Eg~3.37 ev) direct band gab, with a large (60 mev) excitonic binding energy. Zinc oxide (ZnO) has greatly influenced the properties through its growth process, particle size, and especially through morphology [1] [2]. Additionally, ZnO is primarily used as products of personal care, electronics, chemical sensors, solar energy conversion, various luminescence, photo-catalysis and other applications such as sunscreens,

which require UV protection, so ZnO is considered the most common types of metal used in the preparation of NP [3] [4] [5] [6]. Different substrates such as Al_2O_3, silica, carbon and SiO_2 are usually deposited with ZnO to improve its utilization. For example, activated carbon mixtures and ZnO [7] [8] [9] [10], are usually used to obtain ZnO/carbon composites by solution combustion of a single step synthesis [11], and used as an electrode for photocatalytic catalyst and supercapacitor of electrochemical [7] [11]. Also, it can enter the environment via domestic sewage from swimming or showering or through wastewater at industrial sites. Sewage sludge is used (e.g. fertilizer) for land application; it can be used for transporting NP to soil.

In recent days, it was found that ZnO nano-crystallites properties were dramatically changed by surface coating with different semiconductors [12]. Generally, the core-shell structured material synthesis leads to obtain a new composite material having properties between the shell and core materials [13] [14] [15]. One of the potential applications as electroluminescent devices and candidates for the coating materials [16] is ZnS (Zinc sulfide) that has 3.72 eV wide band gap [17]. Gonzalez-Hernandeza *et al.* [18] prepared ZnO nanoparticles doped with fluorine by the precipitation technique and reported the yields of F:ZnO and ZnO. Nano-arrangements consist of different lengths of nanoparticles with ~30 nm chains in size and quasi-spherical in shape. One of the major digestive enzymes in animals is α-amylases, which work on the polysaccharides and break them into small chains (such as starch, the major sugar in the diet, broken by α-amylases into glucose and maltose). When inhibiting α-amylases, there will be less sugar available for assimilation and thus easier to control diabetes. Therefore, α-amylase is used in the design of drugs and the development of compounds used in treatment of obesity, hyperlipidemia and diabetes [19]. When using ZnO nanoparticles to inhibit the α-amylase activity for the first time, it was found that 20 μg/ml optimum dose was sufficient to inhibit 49% of glucose at 35˚C and neutral pH. Inhibition by ZnO nanoparticles is similar to inhibition obtained by acarbose (standard of α-amylase inhibitor), so increment of the production of ZnO nanoparticles is very important as a novel type of amylase inhibitor. Recently, it has been shown that ZnO nanoparticles have function as an active material for bio applications [20] [21] [22] [23] [24] typically as cholesterol biosensors, dietary modulators for hydrolase's activity and antimicrobial agents, due to its high surface to volume ratio [25]. When comparing the precipitation approach method with other traditional methods provides a facile way for large-scale production and low cost, which does not need complicated equipment and expensive raw materials [26], the ability to prepare compounds with varying morphologies having different properties, nontoxicity, existentially found in nature [27]. Therefore, the present study aimed to: 1) synthesize the highly pure ZnONPs and Cl:ZnONPs at different conditions by precipitation technique; 2) examine the antidiabetic activity of ZnONPs and Cl:ZnONPs.

2. Experiment

2.1. Samples Preparation

The method of chemical solution from oxalic acid (OX. acid) and zinc acetate (ZnAc) was used to prepare ZnO nanoparticles doped with chlorine and ZnO nanoparticles. Added OX. acid 0.5 M ethanolic solution (20 mL) drop-by-drop under stirring to ZnAc 0.1 M ethanolic solution (20 mL) and maintained for 1 h and 2 h to prepare (sample: a, b, c, d) at 60˚C. Added to the above solution, ammonium chloride aqueous solution (0.5 M) in order to obtain the ratio of Cl/Zn at 5% to prepare (sample: b and d). A white precipitate was obtained for all samples. Filtrated the samples to separate the precipitates, then washed them by water : ethanol (75:25) mixture. An oven was used to dry the precipitate for 24 h at 100˚C. Finally calcined the obtained precursor for 2 h at 500˚C, with 5˚C/min to prepare ZnO nanoparticles doped with Cl^- (sample: e), added OX. acid 0.5 M ethanolic solution (20 mL) drop-by-drop under stirring to ZnAc 0.1 M ethanolic solution (20 mL) and maintained for 1 h at 60˚C [18].

2.2. Samples Characterization

Fourier Transform Infrared Spectrometer (FTIR) was used to analyze the structure of the samples and IRAFFINITY-1 Shimadzu's in KBr pellets to recorder them in the range of 4000 - 400 cm^{-1}. The crystallinity was assessed by X-ray powder diffractometer (D/max r-B, Rigaku, Japan). Scanning Electron Microscopy (SEM) (Czec Republic, FEI, ISPECT S50) with 20 kV accelerating voltage and Transmutation Electron Microscopy (TEM) (Czec Republic, FEI, TEM) with 80 kV accelerating voltage were used to analyze the Morphology of Surface.

2.3. α-Amylase Inhibitory Assay

The activity of α-amylase inhibitory assayed by the method was described by [28].

3. Results and Discussion

All prepared samples' IR spectra were shown in **Figure 1**. The H–O–H bending vibration and stretching modes were shown at 1650 cm^{-1} and 3500 broad bands of the absorbed or free water. The band observed at 1260 cm^{-1} is attributed to (C-O) + (O-C=O) of –COOH groups of oxalic acid. Strong absorptions at 470 cm^{-1} indicate that the ZnO cluster is formed. Zinc oxide characteristic distinct stretching vibration was shown at 470 cm^{-1}. The hydroxyl group characteristic absorption was indicating at 3400 cm^{-1} broad absorption peak [29]. Moreover, absorption peak of undoped ZnO was observed at 372 nm (3.33 eV), this result agrees with the results reported by Ansari NH *et al.* [30] for ZnO single crystals.

All prepared samples X-ray diffraction (XRD) patterns are shown in **Figure 2**. All Samples exhibited similar patterns indicating high crystallinity. The positioned of diffraction peaks at 2θ values = 31.1˚, 34.4˚, 36˚, 47.1˚, and 56.6˚ were

indicated, which correspond to ZnO planes ((100), (002), (101), (102), and (110)), respectively [4]. Also, this result agrees with the diffraction peaks reported by [4] for zinc oxide hexagonal wurtzite phase in JCPDS card no. 36-1451. From our results, also no other diffraction peaks were noted, therefore, the prepared ZnO are of the pure wurtzite phase. 2θ values of the diffraction peaks which recorded of ZnO = (31.9˚), (34.6˚), (36.4˚), (47.7˚), (56.7˚), (62.9˚), and (68.10), which correspond to diffraction planes: (100), (002), (101), (102), (103), (112) and (201), respectively. It can index these diffraction planes to Zinc and its structure zinc oxide (ZnO) indicating its crystallinity is high [3]. The wurtzite ZnO structure matches very well with all the diffraction peaks (JCPDS card No. 891397), which shows the diffraction peaks as lines in the figure lower side. By using Scherrer's equation, the product exhibits good crystallinity because it has strong diffraction peaks [2].

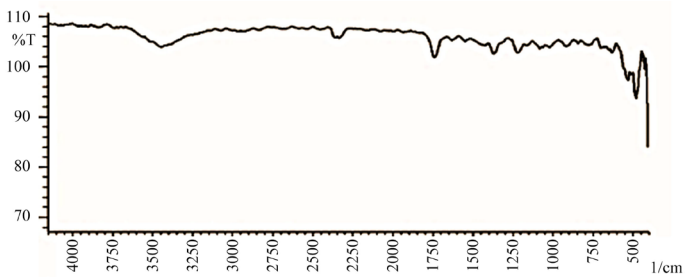

Figure 1. FTIR Spectra of Cl:ZnONPs.

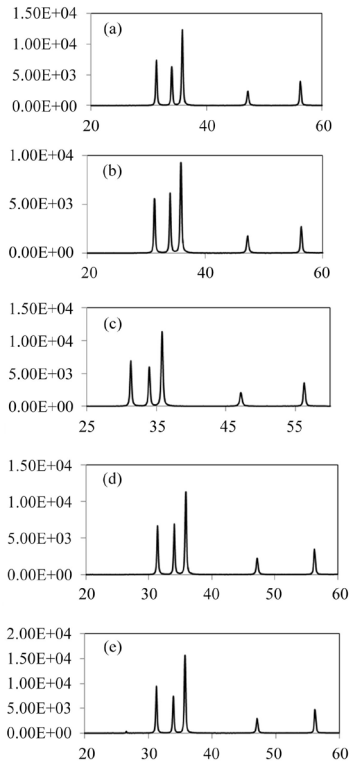

Figure 2. X-ray patterns of: (a) ZnONPs at 1 h, (b) Cl:ZnONPs at 1 h, (c) ZnONPs at 2 h, (d) Cl:ZnONPs at 2 h and (e) Cl:ZnONPs at 1 h.

$$D = \frac{k\lambda}{\beta hkl \cos\theta}$$

$$Dp = 0.94 \times \lambda / (\beta \times \cos\theta)$$

where:

Dp = size of Average Crystallite, θ = Bragg angle, λ = X-ray wavelength for the more intense peaks, β = Line broadening in radians.

Figure 3, **Figure 4** show the morphological characteristics of the ZnONPs and ZnONPs powders prepared with chlorine doping revealed by SEM. ZnONPs at 1 and 2 h (**Figure 3(a)** and **Figure 3(c)**), also Cl:ZnONPs (**Figure 3(b)**) at 1 h show a round shape. On the other hand, Cl:ZnONPs at 2 h (d) and Cl:ZnONPs at 1 h (e) show rode shape. The synthesized nanoparticles have average size 46.65 - 74.64 nm. These results agree with Abd El-Rahman *et al.* [29]. They reported that Cl:ZnONPs show a round shape. The shape difference may be due to the doping nature, the synthesized nanoparticles size is 40 - 50 nm in the range and is nearly spherical in shape. In addition, the particle size determined from analysis of SEM is in good agreement with that of the XRD analysis [29].

Figure 5 (sample a and c) shows ZnO nanoparticles have around 30 nm in round shaped, the amplification in the inset shows that the most particles in the chains are arranged of a length of ~1 μm and other particles are agglomerated. The (samples b, d and e) in **Figure 5** shows the Cl:ZnO nanoparticles TEM images. The prepared powders of ZnO nanoparticles have particle size about 59.3 nm [29]. The analysis of TEM indicated that the ZnONPs particle size varies between 14 and 27 nm, depending on the nanoparticles synthesis method. The ZnONPs morphological characteristics revealed by TEM showed nanocrystalline particles presence and aggregation with various sizes and shapes [31]. Gonzalez-Hernandez, *et al.* [18] reported that Cl:ZnO and ZnONPs have 22 nm and 30 nm particle size, respectively.

The α-amylase inhibitory activity of ZnONPs and Cl:ZnONPs (a-e) at varies concentration from (7.81 to 1000 μM) was studied, **Table 1** and **Figure 6** show the results obtained. The results exhibited a good significant inhibitory activity against α-amylase enzyme of compounds a-c and d when comparable with that of acarbose. Compound (a) showed highly significant inhibition activity (38.11 ± 1.33 and 88.32 ± 0.73)% inhibition at (7.81 and 1000) μM/l concentration, respectively IC50 = 25.54. Compound (c) and (d) showed (37.11 ± 1.2, 30.11 ± 1.38), (42.25 ± 1.5, 35.25 ± 1.22), (47.16 ± 0.63, 45.16 ± 0.53), (59.46 ± 0.58, 53.46 ± 0.68), (63.78 ± 1.2, 59.78 ± 1.29), (69.24 ± 1.5, 61.24 ± 1.56), (76.14 ± 0.63, 69.14 ± 0.69) and (85.32 ± 0.72, 76.32 ± 0.78)% inhibition at (7.81 to 1000) μM/l concentration, respectively, IC50 = (38.47, 49.47) for compound c and d, respectively. Our results agree with Dhobale *et al.* (2008) [32] they reported that; when used ZnO nanoparticles to inhibit the α-amylase activity at the first time, it found that 20 μg/ml optimum dose was sufficient to inhibit 49% of glucose [32].

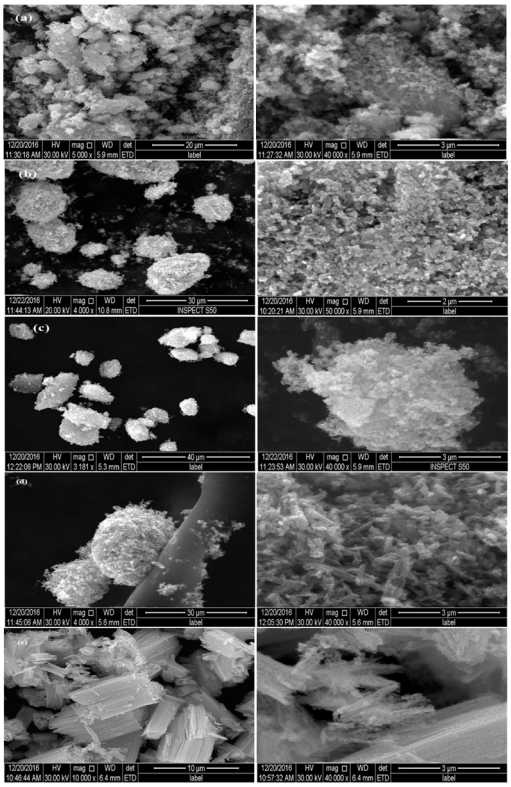

Figure 3. Last two-specimens of low and high magnification SEM images: (a) ZnONPs at 1 h, (b) Cl:ZnONPs at 1 h, (c) ZnONPs at 2 h, (d) Cl:ZnONPs at 2 h and (e) Cl:ZnONPs at 1 h. The surface morphology of the particles is clearly visible at high magnification micrographs. All scale bars correspond to 3 μm (right column).

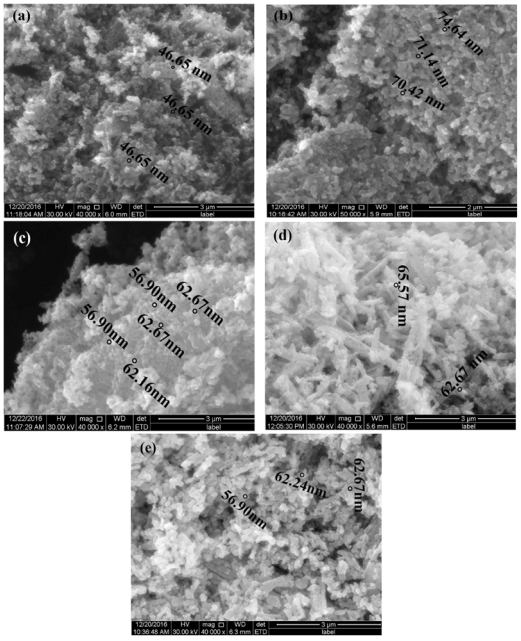

Figure 4. Last two-specimens of low and high magnification SEM images: (a) ZnONPs at 1 h, (b) Cl:ZnONPs at 1 h, (c) ZnONPs at 2 h, (d) Cl:ZnONPs at 2 h and (e) Cl:ZnONPs at 1 h. The surface morphology of the particles is clearly visible at high magnification micrographs. All scale bars correspond to 3 μm (right column).

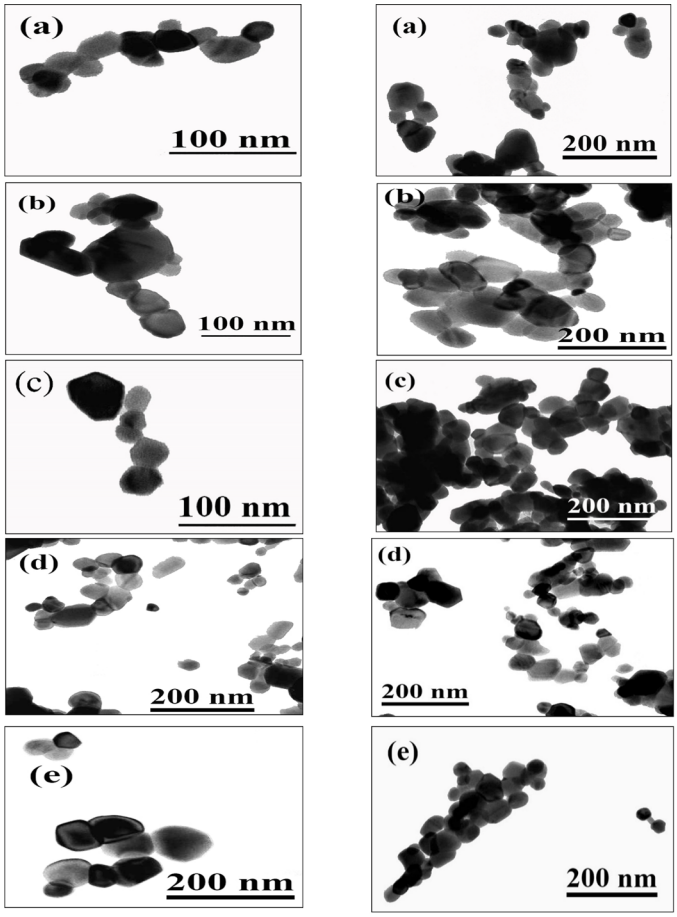

Figure 5. The images of TEM: (a) ZnONPs at 1 h, (b) Cl:ZnONPs at 1 h, (c) ZnONPs at 2 h, (d) Cl:ZnONPs at 2 h and (e) Cl:ZnONPs at 1 h. The surface morphology of the particles is clearly visible at high magnification micrographs. All scale bars correspond to 3 μm (right column).

Table 1. Anti-diabetic activity is depicted in the ZnONPs and Cl:ZnONPs.

Sample conc. (μg)	Control (acarbose)	Sample (a)	Sample (b)	Sample (c)	Sample (d)	Sample (e)
7.81	37.81 ± 1.2	38.11 ± 1.33	0.0 ± 0.0	37.11 ± 1.2	30.11 ± 1.38	21.11 ± 1.44
15.63	40.75 ± 1.5	46.25 ± 1.48	10.46 ± 1.25	42.25 ± 1.5	35.25 ± 1.22	31.25 ± 1.66
31.25	48.84 ± 1.2	52.16 ± 0.59	17.85 ± 0.78	47.16 ± 0.63	45.16 ± 0.53	42.16 ± 0.83
62.5	59.31 ± 1.5	63.46 ± 0.56	24.38 ± 1.37	59.46 ± 0.58	53.46 ± 0.68	47.46 ± 0.68
125	60.17 ± 0.63	69.78 ± 1.32	42.41 ± 0.76	63.78 ± 1.2	59.78 ± 1.29	51.78 ± 1.44
250	69.37 ± 1.2	71.24 ± 1.44	57.32 ± 1.53	69.24 ± 1.5	61.24 ± 1.56	55.24 ± 1.49
500	80.14 ± 0.58	79.14 ± 0.65	63.34 ± 1.82	76.14 ± 0.63	69.14 ± 0.69	62.14 ± 0.73
1000	86.32 ± 0.63	88.32 ± 0.73	69.21 ± 1.44	85.32 ± 0.72	76.32 ± 0.78	69.3 ± 20.82
IC 50	34.71	25.54	188.63	38.47	49.47	99.25

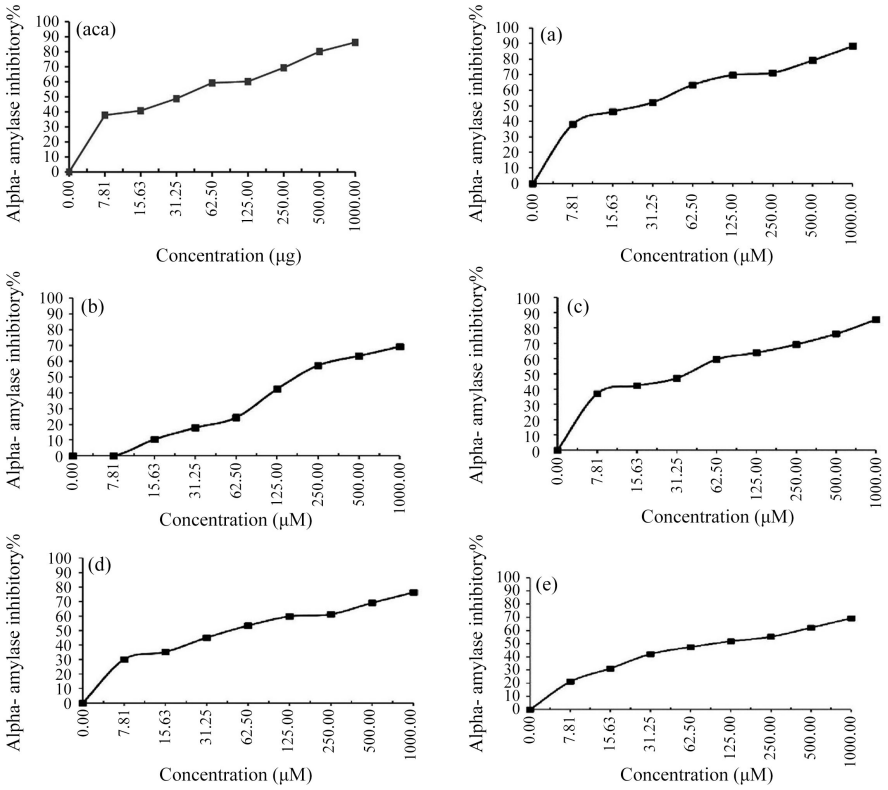

Figure 6. *α*-Amylase inhibitory assay test for (a) ZnONPs at 1 h, (b) Cl:ZnONPs at 1 h, (c) ZnONPs at 2 h, (d) Cl:ZnONPs at 2 h and (e) Cl:ZnONPs at 1 h.

4. Conclusion

ZnONPs and Cl:ZnONPs were elucidated as *α*-amylase inhibitors. Compound (c) shows the best inhibitory activity than other compounds except compound (a) when compared with the standard of *α*-amylase (acarbose). Moreover, compound (a) gives the highest inhibitor activity than acarbose. So we concluded that the present results, considered as beginning to pave the way to identify a new material (Cl:ZnONPs), can be used in the treatment of chronic diseases such as diabetes in the field of biomedicine.

Acknowledgements

The author extends their sincere thanks to the Institute for Research and Medical Consultations (IRMC) and research units of Science College in Imam Abdulrahman Bin Faisal University.

Conflicts of Interest

The authors declare no conflicts of interest regarding the publication of this paper.

References

[1] Zhang, J., Yu, W.Y. and Zhang, L.D. (2002) Fabrication of Semiconducting ZnO

Nanobelts Using a Halide Source and Their Photoluminescence Properties. *Physics Letters A*, **299**, 276-281. https://doi.org/10.1016/S0375-9601(02)00622-9

[2] Chen, Y.X., Zhao, X.Q. and Chen, J.H. (2008) Stacking Fault Directed Growth of Thin ZnO Nanobelt. *Materials Letters*, **62**, 2369-2371. https://doi.org/10.1016/j.matlet.2007.12.004

[3] Sun, T.J., Qiu, J.S. and Liang, C.G. (2008) Controllable Fabrication and Photocatalytic Activity of ZnO Nanobelt Arrays. *The Journal of Physical Chemistry C*, **112**, 715-721. https://doi.org/10.1021/jp710071f

[4] Cao, B.Q., Teng, X.M., Heo, S.H., Li, Y., Cho, S.O., Li, G.H. and Cai, W.P. (2007) Different ZnO Nanostructures Fabricated by a Seed-Layer Assisted Electrochemical Route and Their Photoluminescence and Field Emission Properties. *The Journal of Physical Chemistry C*, **111**, 2470-2476. https://doi.org/10.1021/jp066661l

[5] Kong, X.Y., Ding, K. and Wang, Z.L. (2004) Metal-Semiconductor Zn-ZnO Core-Shell Nanobelts and Nanotubes. *The Journal of Physical Chemistry C*, **108**, 570-574. https://doi.org/10.1021/jp036993f

[6] Reynolds, D.C., Look, D.C., Jogai, B., Hoelscher, J.E., Sherriff, R.E., Harris, M.T. and Callahan, M.J. (2000) Time-Resolved Photoluminescence Lifetime Measurements of the Γ5 and Γ6 Free Excitons in ZnO. *Journal of Applied Physics*, **88**, Article No. 2152. https://doi.org/10.1063/1.1305546

[7] Kalpana, D., Omkumar, K.S., Kumar, S.S. and Renganathan, N.G. (2006) A Novel High Power Symmetric ZnO/Carbon Aerogel Composite Electrode for Electrochemical Supercapacitor. *Electrochimica Acta*, **52**, 1309-1315. https://doi.org/10.1016/j.electacta.2006.07.032

[8] Sobana, N., Muruganandam, M. and Swaminathan, M. (2008) Characterization of Ac-ZnO Catalyst and Its Photocatalytic Activity on 4-Acetylphenol Degradation. *Catalysis Communications*, **9**, 262-268. https://doi.org/10.1016/j.catcom.2007.04.040

[9] Sobana, N. and Swaminathan, M. (2007) Combination Effect of ZnO and Activated Carbon for Solar Assisted Photocatalytic Degradation of Direct Blue 53. *Solar Energy Materials and Solar Cells*, **91**, 727-734. https://doi.org/10.1016/j.solmat.2006.12.013

[10] Byrappa, K., Subramani, A.K., Ananda, S., Lokanatharai, K.M., Suntha, M.H., Basavalingu, B. and Soga, K. (2006) Impregnation of ZnO onto Activated Carbon under Hydrothermal Conditions and Its Photocatalytic Properties. *Journal of Materials Science*, **41**, 1355-1362. https://doi.org/10.1007/s10853-006-7341-x

[11] Jayalakshmi, M., Palaniappa, M. and Balasubramanian, K. (2008) Single Step Solution Combustion Synthesis of ZnO/Carbon Composite and Its Electrochemical Characterization for Supercapacitor Application. *International Journal of Electrochemical Science*, **3**, 96-103.

[12] Sadollahkhani, A., Kazeminezhad, I., Lu, J., Nur, O., Hultman L. and Willander, M. (2014) Synthesis, Structural Characterization and Photocatalytic Application of ZnO@ZnS Core-Shell Nanoparticles. *RSC Advances*, **4**, 36940-36950. https://doi.org/10.1039/C4RA05247A

[13] Reiss, P., Protiere, M. and Li, L. (2009) Core/Shell Semiconductor Nanocrystals. *Small*, **5**, 154-168. https://doi.org/10.1002/smll.200800841

[14] Zeng, Z., Garoufalis, C.S., Terzis, A.F. and Baskoutas, S. (2013) Linear and Nonlinear Optical Properties of ZnO/ZnS and ZnS/ZnO Core Shell Quantum Dots: Effects of Shell Thickness, Impurity, and Dielectric Environment. *Journal of Applied Physics*, **114**, Article ID: 23510. https://doi.org/10.1063/1.4813094

[15] Zhai, J., Tao, X., Pu, Y., Zeng, X.F. and Chen, J.F. (2010) Structured ZnO/SiO_2 Nanoparticles: Preparation, Characterization and Photocatalytic Property. *Applied Surface Science*, **257**, 393-397. https://doi.org/10.1016/j.apsusc.2010.06.091

[16] Sahare, S., Dhoble, S.J., Singh, P. and Ramrakhiani, M. (2013) Fabrication of ZnS:Cu/PVA Nanocomposite Electroluminescence Devices for Flat Panel Displays. Advanced Materials Letter, **4**, 169-173. https://doi.org/10.5185/amlett.2012.6374

[17] Roychowdhury, A., Pati, S.P., Kumar, S. and Das, D. (2014) Effects of Magnetite Nanoparticles on Optical Properties of Zinc Sulfide in Fluorescent-Magnetic Fe_3O_4/ZnS Nanocomposites. *Powder Technology*, **254**, 583-590. https://doi.org/10.1016/j.powtec.2014.01.076

[18] Gonzalez-Hernandez, R., Martinez, A.I., Falcny, C.A., Lopez, A., Pech-Canul, M.I. and Hdz-Garcia, H.M. (2010) Study of the Properties of Undoped and Fluorine Doped Zinc Oxide Nanoparticles. *Materials Letters*, **64**, 1493-1495. https://doi.org/10.1016/j.matlet.2010.04.001

[19] Franco, O.L., Rigden, D.J., Melo, F.R., Bloch Jr., C., Silva, C.P. and Grossi de Sá, M.F. (2000) Activity of Wheat α-Amylase Inhibitors towards Bruchid α-Amylases and Structural Explanation of Observed Specificities. *European Journal of Biochemistry*, **267**, 2166-2173. https://doi.org/10.1046/j.1432-1327.2000.01199.x

[20] Khan, R., Kaushik, A., Solanki, P.R., Ansari, A.A., Pandey, M.K. and Malhotra, B.D. (2008) Zinc Oxide Nanoparticles-Chitosan Composite Film for Cholesterol Biosensor. *Analytica Chimica Acta*, **616**, 207-213. https://doi.org/10.1016/j.aca.2008.04.010

[21] Reddy, K.M., Feris, K., Bell, J., Wingett, D.G., Hanley, C. and Punnoose, A. (2007) Selective Toxicity of Zinc Oxide Nanoparticles to Prokaryotic and Eukaryotic Systems. *Applied Physics Letters*, **90**, Article ID: 213902. https://doi.org/10.1063/1.2742324

[22] Szabo, J., Hegedus, M., Bruckner, G., Kosa, E., Andrasofszky, E. and Berta, E. (2004) Large Doses of Zinc Oxide Increases the Activity of Hydrolases in Rats. *The Journal of Nutritional Biochemistry*, **15**, 206-209. https://doi.org/10.1016/j.jnutbio.2003.09.005

[23] Bárcena, C., Sra, A.K., Chaubey, G.S., Khemtong, C., Liu, J.P. and Gao, J. (2008) Zinc Ferrite Nanoparticles as MRI Contrast Agents. *Chemical Communications*, **19**, 2224-2226. https://doi.org/10.1039/b801041b

[24] Xiong, H.M., Xu, Y., Ren, Q.G. and Xia, Y.Y. (2008) Stable Aqueous ZnO@Polymer Core-Shell Nanoparticles with Tunable Photoluminescence and Their Application in Cell Imaging. *Journal of the American Chemical Society*, **130**, 7522-7523. https://doi.org/10.1021/ja800999u

[25] Das, D., Nath, B.C., Phukon, P., Kalita, A. and Dolui, S.K. (2013) Synthesis of ZnO Nanoparticles and Evaluation of Antioxidant and Cytotoxic Activity. *Colloids and Surfaces B*: *Biointerfaces*, **111**, 556-560. https://doi.org/10.1016/j.colsurfb.2013.06.041

[26] Wang, C., Zhang, W.X., Qian, X.F., Zhang, X.M., Xie, Y. and Qian, Y.T. (1999) A Room Temperature Chemical Route to Nanocrystalline PbS Semiconductor. *Materials Letters*, **40**, 255-258. https://doi.org/10.1016/S0167-577X(99)00085-3

[27] Nagajyothi, P.C., Cha, S.J., Yang, I.J., Sreekanth, T.V.M., Kim, K.J. and Shin, H.M. (2015) Antioxidant and Anti-Inflammatory Activities of Zinc Oxide Nanoparticles Synthesized Using *Polygala tenuifolia* Root Extract. *Journal of Photochemistry and Photobiology B*: *Biology*, **146**, 10-17. https://doi.org/10.1016/j.jphotobiol.2015.02.008

[28] Funke, I. and Melzig, M.F. (2006) Traditionally Used Plants in Diabetes Thera-

py—Phytotherapeutics as Inhibitors of a-Amylase Activity. *Revista Brasileira de Farmacognosia*, **16**, 1-5. https://doi.org/10.1590/S0102-695X2006000100002

[29] Abd El-Rahman, S.N., Reda, S.M. and Al Ghannam, S.M. (2016) Synthesis and Characterization of Nano-Doped Zinc Oxide and Its Application as Protective Oxidative Changes in the Retina of Diabetic Rats. *Journal of Diabetes & Metabolism*, **7**, Article No. 691. https://doi.org/10.4172/2155-6156.1000691

[30] Ansari, N.H., Zhang, W., Fulep, E. and Mansour, A. (1998) Prevention of Pericyte loss by Trolox in Diabetic Rat Retina. *Journal of Toxicology and Environmental Health*, *Part A*, **54**, 467-475. https://doi.org/10.1080/009841098158755

[31] El Saeed, A.M., Abd El-Fattah, M. and Azzam, A.M. (2015) Synthesis of ZnO Nanoparticles and Studying Its Influence on the Antimicrobial, Anticorrosion and Mechanical Behavior of Polyurethane Composite for Surface Coating. *Dyes and Pigments*, **121**, 282-289. https://doi.org/10.1016/j.dyepig.2015.05.037

[32] Dhobale, S., Thite, T., Laware, S.L., Rode, C.V., Koppikar, S.J., Ruchika-Kaul, G. and Kale, S.N. (2008) Zinc Oxide Nanoparticles as Novel Alpha-Amylase Inhibitors. *Journal of Applied Physics*, **104**, Article ID: 094907. https://doi.org/10.1063/1.3009317